Journal of Power Sources 249 (2014) 457–462

Contents lists available at ScienceDirect

Journal of Power Sources

journal homepage: www.elsevier.com/locate/jpowsour

State of health estimation for lithium ion batteries based on charging curves

Zhen Guo [a], Xinping Qiu [b], Guangdong Hou [a], Bor Yann Liaw [c], Changshui Zhang [a,*]

[a] State Key Laboratory of Intelligent Technologies and Systems, Tsinghua National Laboratory for Information Science and Technology (TNList), Department of Automation, Tsinghua University, Beijing 100084, China
[b] Key Laboratory of Organic Optoelectronics and Molecular Engineering, Department of Chemistry, Tsinghua University, Beijing 100084, China
[c] Hawaii Natural Energy Institute, SOEST, University of Hawaii at Manoa, Honolulu, HI 96822, USA

HIGHLIGHTS

- An adaptive curve transformation is used to quantify the battery capacity fade.
- Only one "time-based" parameter is needed in the model to enable SOH estimation.
- Only the initial charging data is needed to train the estimation model.
- The SOH estimation accuracy is not affected by duty cycles or aging history.

ARTICLE INFO

Article history:
Received 30 August 2013
Accepted 24 October 2013
Available online 7 November 2013

Keywords:
State of health
Lithium ion battery
Charge curve
Nonlinear least squares method

ABSTRACT

An effective method to estimate the state of health (SOH) of lithium ion batteries is illustrated in this work. This method uses an adaptive transformation of charging curves at different stages of life to quantify the extent of capacity fade and derive a time-based parameter to enable an accurate SOH estimation. This approach is easy for practical implementation and universal to chemistry or cell geometry, with minimal demand of learning. With a typical constant current–constant voltage (CC–CV) charging method for a lithium ion battery, this approach uses an equivalent circuit model to characterize the CC portion of the charging curve and derive a transformation function and a time-based parameter to estimate SOH at any stage of life via a nonlinear least squares method to identify model parameters. The SOH estimation errors (discrepancy between estimated and experimental values, denoted as ΔSOH) are under 2% before the end of life in cases shown at 25 °C and 60 °C and a range of typical discharging rates up to 3C. With different sizes and chemistries, the ΔSOHs are all less than 3%.

1. Introduction

Lithium ion batteries (LIBs) are widely used in portable electronic products and new energy technologies such as electric vehicles and electrical energy storage systems. They have some incomparable advantages compared to other rechargeable batteries, including higher energy density, less maintenance requirement, higher nominal voltage, lower self-discharge rate; thus, LIB is regarded as one of the most promising energy solutions. However, its performance degrades with time because of impacts from operating environment and aging history. The battery failure may result in serious, sometimes catastrophic, consequences. Therefore, it is desirable to estimate the state of health (SOH) of the battery to predict how soon it will fail or void the guarantee of satisfactory performance.

Extensive studies have been carried out for the SOH estimation in recent years. Some consider SOH estimation as a black-box problem, using artificial intelligence (AI) and machine learning (ML) to estimate SOH for various operating conditions without full understanding of the aging mechanism. AI and ML algorithms including support vector machine (SVM), probabilistic neural network (PNN), recurrent neural network (RNN), and fuzzy identification have been employed in various attempts for SOH estimation [1–5]. However, a sufficient amount of test data must be obtained to train the estimation model, and proper estimation methods and algorithms are crucial for implementation. There are other attempts to develop numerical models to describe battery aging behavior in mathematical formulae, equivalent circuit

* Corresponding author.
E-mail address: zcs@mail.tsinghua.edu.cn (C. Zhang).

0378-7753/$ – see front matter © 2013 Elsevier B.V. All rights reserved.
http://dx.doi.org/10.1016/j.jpowsour.2013.10.114

diagrams, or electrochemical equations [6–9]. In these models, specific parameter identification techniques are used to correlate electrochemical properties in the LIB with degradation, and the SOH is reflected by one parameter or combinatory variants determined using parameter identification techniques. In Refs. [6,7], simple equivalent circuit models (ECM) were proposed to support parameter identification methodology. The internal resistance and open circuit voltage (OCV) were used in the parameterization. In Refs. [8,9], electrochemical-based single particle model (SPM) were proposed, and a nonlinear least squares method was used for parameterization. These approaches mentioned above mostly derive qualitative SOH estimation based on state of charge (SOC), impedance, or OCV, which is not as user-friendly as expected in actual operations.

In this paper, an effective SOH estimation method for single cells of LIB is proposed. The same approach can be applied to multi-cell systems, although it is not demonstrated here. This approach can facilitate easier implementation, less demand for prior learning, and better generalization to accommodate variations in cell design and chemistry. Some important aspects of this approach are denoted here:

1. The voltage–time data in the constant-current (CC) step of the charging profile are adopted in this approach due to the following considerations: (1) in practical use, the charging process is executed in a more controlled manner in contrast to discharging process under a duty cycle; (2) the voltage–time variables are easy to measure than the others such as resistance, OCV, SOC et al.; and, (3) the constant-voltage (CV) step in the charging profile is not considered because it's more time consuming and inconvenient in data collection and analysis.
2. To deduce SOH estimation mathematical model, the voltage variations with time in the CC step of the charging profile are characterized as a function of aging duration. A typical ECM used by many others is introduced to derive aging parameters for the SOH estimation. Among all necessary model parameters, only a "time-based" one is used in the model formula to enable SOH estimation; avoiding the use of OCV or SOC as variables in the estimation process, due to the difficulty in deriving these variables in practical use. This unique aspect offers very attractive and favorable operability in actual implementation.
3. Only the initial charging curve as a benchmark of a fresh battery to represent the chemistry in the cell, corresponding to the 100% SOH, is needed in this model and the initial model parameterization is learned with regression algorithm from the voltage–time offline data in the CC step. With the aging of the battery, the SOH can be quantified by the unique time-based parameter in the estimation model formula, and the parameters identification is realized by a nonlinear least squares method.
4. As long as the operating limits of voltage, current, and temperature are not exceeded, the voltage profile with the same charging current can reflect the aging of the battery and the variation of such voltage profile with aging can be quantified through a continuous update of the time-based parameter. In other words, the accuracy of the estimation model is not affected by duty cycles or complicated aging history; thus, the applicability of this SOH estimation method is quite universal and very easy to implement.

2. Mathematical model for SOH estimation

2.1. Model description

Fig. 1(a) shows the charging profiles of a $LiCoO_2/LiNi_xMn_yCo_zO_2$-based LIB at 100%, 95%, 90%, 85%, and 80% SOH, respectively. These

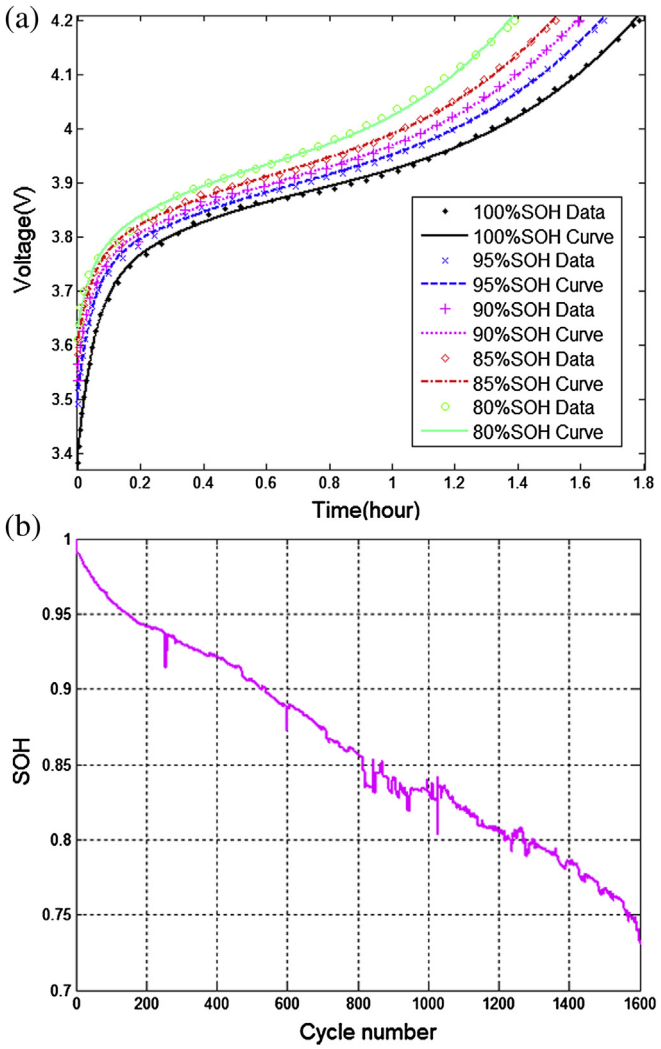

Fig. 1. (a) Charging curves of a $LiCoO_2/LiNi_xMn_yCo_zO_2$-based LIB at 100%, 95%, 90%, 85%, and 80% *SOHs*. Typical CC–CV charging method is used and only the CC profiles at C/2 are shown. (b) The corresponding *SOH* curve as a function of cycle number.

profiles were recorded using a typical CC–CV charging method, but only the CC profiles are shown. Fig. 1(b) exhibits the SOH changes with cycle number. Intuitively, these charging curves are similar to one another, progressively shifting to a shorter time span and higher voltage range with cycle number. Such a trend inspires this approach of SOH estimation.

These CC charging profiles can be represented properly with an ECM [6,7,10] (Fig. 2). The ECM consists of an ohmic resistor (R_Ω), a parallel *RC* network (R_p and C_p), and a voltage source (U_{oc}). The R_Ω represents a physical resistive effect in the dynamics of the battery kinetic behavior, which is responsible for the instantaneous IR

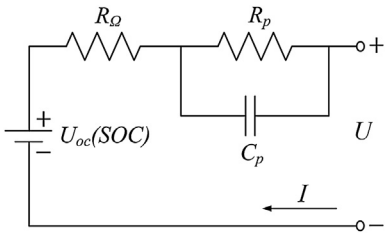

Fig. 2. A simple ECM of LIB.

voltage drop in the charging or discharging process upon polarization. The parallel R_p–C_p network describes the nonlinear, faradic charge–transfer impedance of a battery. $U_{oc}(SOC)$ is the equilibrium OCV of the battery, increasing nonlinearly and monotonously with SOC. U is the battery terminal voltage and I the current under polarization. Two assumptions associated with ECM are given below to simplify the illustration in the discussion:

1. R_Ω, R_p, and C_p are invariant in the operating range (e.g. 3.0–4.2 V), and they change with aging of the battery.
2. $U_{oc}(SOC)$ is only associated with SOC within certain error tolerance [11]. The $U_{oc}(SOC)$ curve is also considered invariant in the temperature range and aging process during operation.

During CC charging the battery voltage can be expressed by a nonlinear function with variables SOC and time t as

$$\begin{aligned} U(SOC,t) &= U_{oc}(SOC) - U_p\cdot\exp^{-\frac{t}{\tau}} + I\cdot R_p\left(1-\exp^{-\frac{t}{\tau}}\right) + I\cdot R_\Omega \\ &= U_{oc}(SOC) - (U_p + I\cdot R_p)\exp^{-\frac{t}{\tau}} + I\cdot(R_p + R_\Omega) \end{aligned} \quad (1)$$

Where $\tau = R_p\cdot C_p$, U_p the polarization voltage when $t = 0$, and all variables positive.

In Eq. (1), the relation between SOC and t can be further established by introducing the recharged capacity C_r, stored capacity C_s, and usable capacity C_u. The C_r represents the capacity obtained from the CC charging step started from $t = 0$. The C_s represents the remaining capacity after the last discharging, and the C_u represents the actual or usable capacity as the results of aging. All of above can be described by Eq. (2)

$$SOC = \frac{C_r + C_s}{C_u} = \frac{I\cdot t + C_s}{C_u} \quad (2)$$

Accordingly, Eq. (1) can be rewritten as

$$U(SOC,t) = U_{oc}(SOC) - (U_p + I\cdot R_p)\exp^{-\frac{C_u}{\tau\cdot I}\cdot\frac{(I\cdot t + C_s - C_s)}{C_u}} + I\cdot(R_p + R_\Omega) \quad (3)$$

The battery voltage as a function of SOC can be expressed as

$$U(SOC) = U_{oc}(SOC) - (U_p + I\cdot R_p)\exp^{-\frac{C_u}{\tau\cdot I}\cdot SOC}\cdot\exp^{\frac{C_s}{\tau\cdot I}} + I\cdot(R_p + R_\Omega) \quad (4)$$

with the cycle number increasing, C_u will degenerate gradually. At a certain state of aging, C_u is denoted as C'_u. Accordingly, the parameters U, U_p, R_p, R_Ω, C_s, and τ in Eq. (4) are deformed as U', U'_p, R'_p, R'_Ω, C'_s, and τ'. On the premise of assumptions 1 and 2, Eq. (4) can be rewritten to describe the change of the battery voltage as

$$U'(SOC) = U_{oc}(SOC) - \left(U'_p + I\cdot R'_p\right)\exp^{-\frac{C}{\tau'\cdot I}\cdot SOC}\cdot\exp^{\frac{C'_u}{\tau'\cdot I}} + I\left(R'_p + R'_\Omega\right) \quad (5)$$

According to Eqs. (4) and (5), the voltage diversity with variable SOC is expressed as

$$\begin{aligned} U'(SOC) - U(SOC) = {} & (U_p + I\cdot R_p)\exp^{-\frac{C_u}{\tau\cdot I}\cdot SOC}\cdot\exp^{\frac{C_s}{\tau\cdot I}} \\ & - \left(U'_p + I\cdot R'_p\right)\exp^{-\frac{C'_u}{\tau'\cdot I}\cdot SOC}\cdot\exp^{\frac{C'_s}{\tau'\cdot I}} \\ & + I\left(R'_p + R'_\Omega\right) - I(R_p + R_\Omega) \end{aligned} \quad (6)$$

It is important to note that in Eq. (6), $U_{oc}(SOC)$ is not present, which eliminates its exhausting requirement for measurement in practice. This aspect solved the dilemma often experienced in BMS where the $U_{oc}(SOC)$ is difficult to measure or estimate. However, in Eq. (6) another dilemma in dealing with SOC remains. SOC is difficult to handle because the parameter cannot be determined directly or estimated easily with certainty. To resolve this issue, Eq. (2) shall be used to represent SOC in Eq. (6). Eq. (6) can now be rewritten as

$$\begin{aligned} U'(t') = {} & U(t) + (U_p + I\cdot R_p)\exp^{-\frac{1}{\tau}\cdot t} - \left(U'_p + I\cdot R'_p\right)\exp^{-\frac{1}{\tau'}\cdot t'} \\ & + I\left(R'_p + R'_p\right) - I(R_p + R_\Omega) \end{aligned} \quad (7)$$

$$t = \frac{C_u}{C'_u}\left(t' + \frac{C'_s}{I}\right) - \frac{C_s}{I} \quad (8)$$

where t' corresponds to t at the same SOC, but at a different age.

If the $U(t)$ is obtained from a fresh battery at SOH = 100%, $C_s \approx 0$, the SOH estimation can be deduced from Eqs. (7) and (8) through a further simplification as follows: by making $k = C_u/C'_u$, $\Delta t = C'_s/I$, $a = U_p + I\cdot R_p$, $b = -1/\tau$, $c = U'_p + I\cdot R'_p$, $d = -1/\tau'$, $e = I(R'_p + R'_\Omega - R_p - R_\Omega)$ a universal mathematical expression is derived as

$$U'(t') = U(k(t' + \Delta t)) + a\cdot\exp^{b\cdot k(t'+\Delta t)} - c\cdot\exp^{d\cdot t'} + e \quad (9)$$

The parameters (k, Δt, a, b, c, d, and e) in Eq. (9) can be identified by using a numerical calculation method to yield an estimation of k. The SOH can then be represented as $1/k$.

2.2. Parameter identification procedure

As a LIB ages, its capacity fades, as indicated by the gradually shortened span in the charging profile under the same charging condition and the rising cell voltage at the same capacity as shown in Fig. 1(a). This gradual change in the charging profile as a function of battery aging makes it possible to use the change in voltage–time curves to estimate SOH and battery's remaining service life.

To perform parameter identification, we shall start with the first charge/discharge cycle of a fresh LIB cell as a baseline. The CC charging profile is denoted as (U, t). By using a nonlinear least squares method, a single-variable function $U(t)$ is obtained to represent this CC charging profile and used it as a benchmark for 100% SOH. The parameters a and b should be identified first. In the parameterization process, several constraints, including $k \to 1$, $\Delta t \to 0$ and $e \to 0$, must be met. Once that $a \approx c$ and $b \approx d$ were found, the process terminated, and a and b were determined.

For a charging profile at any age of life, it can be represented as (U', t'), according to Eq. (9), with all parameters fit by the nonlinear least squares method. As the battery ages, the voltage–time data sets (U', t') shall be updated, and only five parameters (i.e. k, Δt, c, d, e) in Eq. (9) shall be considered in the iteration.

3. Experimental

Six commercial LIBs (No. 1–6) made for electronic products were tested for cycle aging experiments. When the nominal capacity faded to 80% of the rated capacity, the test was terminated and charge/discharge data analyzed. The test schemes are formulated as follows:

3.1. Test scheme 1

Three new 2.2Ah LS-18650 ($LiCoO_2/LiNi_xMn_yCo_zO_2$) batteries (No. 1–3) were charged using a typical CC–CV method where CC = C/2 with an end-of-charge voltage EOCV = 4.2 V and

CV = 4.2 V with an end-of-charge current EOCC = C/20. In the discharging tests, the end-of-discharge voltage EODV = 3.0 V is used. Battery No. 2 was subjected to 60 °C test, while No. 1 and 3 were tested at 25 °C. Battery No. 3 was subjected to test with a discharge current DC = 3C without rest interval, while No. 1 and 2 were discharged at 1 C with 10 min rest interval between charge and discharge regimes. The detailed test conditions for each battery are specified in Table 1. As Li plating may occur during low-temperature charging [12] and lead to additional battery degradation, low-temperature tests were not considered in this work.

3.2. Test scheme 2

Battery No. 4 (LS-18650), No. 5 (EVE-402030) and No. 6 (TJ-18650) with different cathode compositions and capacity ratings were tested at room temperature using conditions listed in Table 2. All subjected to CC = 1C and DC = 1C, and a rest interval of 10 min was applied between charge and discharge regimes.

4. Results and discussion

4.1. Model extraction

In Test scheme 1, the benchmark charging profile at 100% SOH was produced from the first cycle of battery No. 1, and its function is denoted as $U(t)_{LS1}$. For battery No. 4–6 in Test scheme 2, the benchmark charging profile functions are denoted respectively as $U(t)_{LS2}$, $U(t)_{EVE}$, and $U(t)_{TJ}$. Four function formula were extracted, following the procedures described in Refs. [13], as follows:

$$U(t)_{LS1} = -0.30\cdot exp^{-18.77\cdot t} + 0.42\cdot t - 0.35\cdot t^2 + 0.15\cdot t^3 + 3.71 \quad (10)$$

$$U(t)_{LS2} = -0.35\cdot \exp^{-46.02\cdot t} + 1.22\cdot t - 2.20\cdot t^2 + 1.81\cdot t^3 + 3.70 \quad (11)$$

$$U(t)_{EVE} = -0.10\cdot \exp^{-113.00\cdot t} + 0.83\cdot t - 1.35\cdot t^2 + 1.20\cdot t^3 + 3.78 \quad (12)$$

$$U(t)_{TJ} = -0.55\cdot \exp^{-4.10\cdot t} - 1.12\cdot t + 1.30\cdot t^2 - 0.22\cdot t^3 + 4.10 \quad (13)$$

Using the method described in Section 2, parameters a and b in Eq. (9) were identified by fitting the benchmark charging profiles respectively for each battery. The SOH estimation using the mathematical model, denoted as $U'(t')_{LS1}$, $U'(t')_{LS2}$, $U'(t')_{EVE}$, and $U'(t')_{TJ}$ respectively, can be extracted as shown below:

$$\begin{aligned} U'(t')_{LS1} = {} & -0.30\cdot \exp^{-18.77\cdot k(t'+\Delta t)} + 0.42\cdot k(t'+\Delta t) \\ & - 0.35\cdot k^2(t'+\Delta t)^2 + 0.15\cdot k^3(t'+\Delta t)^3 + 3.71 \\ & + 0.52\cdot \exp^{-2.47\cdot k(t'+\Delta t)} - c\cdot \exp^{d\cdot t'} + e \end{aligned} \quad (14)$$

Table 1
Partial specifications of Test scheme 1.

No.	Types	Cathode	Capacity	CC	DC	Int. time	Temp.
1	LS-18650	$LiCoO_2/LiNi_xMn_yCo_zO_2$	2200 mAh	0.5 C	1 C	10 min	25 °C
2	LS-18650	$LiCoO_2/LiNi_xMn_yCo_zO_2$	2200 mAh	0.5 C	1 C	10 min	60 °C
3	LS-18650	$LiCoO_2/LiNi_xMn_yCo_zO_2$	2200 mAh	0.5 C	3 C	0	25 °C

Table 2
Partial specifications of Test scheme 2.

No.	Types	Cathode	Capacity	CC	EOCV	EOCC	EODV
4	LS-18650	$LiCoO_2/LiNi_xMn_yCo_zO_2$	2200 mAh	1C	4.2 V	0.05 C	3.0 V
5	EVE-402030	$LiCoO_2$	190 mAh	1C	4.2 V	0.02 C	3.0 V
6	TJ-18650	$LiNi_xMn_yCo_zO_2$	1000 mAh	1C	4.3 V	0.05 C	2.7 V

$$\begin{aligned} U'(t')_{LS2} = {} & -0.35\cdot \exp^{-46.02\cdot k(t'+\Delta t)} + 1.22\cdot k(t'+\Delta t) \\ & - 2.20\cdot k^2(t'+\Delta t)^2 + 1.81\cdot k^3(t'+\Delta t)^3 + 3.70 \\ & + 0.52\cdot \exp^{-1.31\cdot k(t'+\Delta t)} - c\cdot \exp^{d\cdot t'} + e \end{aligned} \quad (15)$$

$$\begin{aligned} U'(t')_{EVE} = {} & -0.10\cdot \exp^{-113.00\cdot k(t'+\Delta t)} + 0.83\cdot k(t'+\Delta t) \\ & - 1.35\cdot k^2(t'+\Delta t)^2 + 1.20\cdot k^3(t'+\Delta t)^3 + 3.78 \\ & + 0.57\cdot \exp^{-0.21\cdot k(t'+\Delta t)} - c\cdot \exp^{d\cdot t'} + e \end{aligned} \quad (16)$$

$$\begin{aligned} U'(t')_{TJ} = {} & -0.55\cdot \exp^{-4.10\cdot k(t'+\Delta t)} - 1.12\cdot k(t'+\Delta t) \\ & + 1.30\cdot k^2(t'+\Delta t)^2 - 0.22\cdot k^3(t'+\Delta t)^3 + 4.10 \\ & + 0.91\cdot \exp^{-0.01\cdot k(t'+\Delta t)} - c\cdot \exp^{d\cdot t'} + e \end{aligned} \quad (17)$$

4.2. Validation analysis

The SOH estimation model expressed by Eq. (14) is used for batteries No. 1–3 to estimate the SOH through cycle aging, respectively. The error in estimation ($SOH_{est.}$) against experimental data ($SOH_{exp.}$) is illustrated in Fig. 3. The maximum error (discrepancy between estimation and experiment, $\Delta SOH = SOH_{est.} - SOH_{exp.}$) is mostly below 2%. For batteries No. 4–6, with each estimation model shown in Eqs. 15–17 respectively, the results are shown in Fig. 4, with the maximum error below 3%.

There are additional aspects that are worth noting here. The noticeable fluctuations in error (some >2%) around 800–950 cycles in Fig. 3(a) were likely caused by excessive noise from the experimental data, not by the model inaccuracy. The origins of these fluctuations are not clear. However, it is worth noting that after such a period, the trend line of the error function settled around 1% level, breaking away from the original trend of increase. Additional analysis is in progress to investigate if this transition in the trend line has any physical implication due to causality from the test conditions or battery's properties. Fig. 3(b) shows the model follows experimental data well, including a rapid descend in SOH in the vicinity of 500 cycles. Such an illustration is a favorable sign to show the viability of the model prediction. However, one should be cautioned to use this sensitivity in predictability mindfully to avoid being deceived by artifacts. In Fig. 3(c), once the SOH falls below 80%, the capacity fade fluctuates intensively; so is error function. In this region, ΔSOH is close to 4% and seems to increase progressively. The reason is not clear and additional investigation is under way.

The examples in Fig. 4 illustrate the model is capable of estimating SOH in different cell designs and chemistries with a reasonable level of error spreading around 2–3%. In these cases, the charging rate has been increased from C/2 used in the previous samples to 1C. Although it is marginal to imply if a higher charging rate such as 1C would lead to such an increase in error from 2% to 3%, it is nonetheless worth noting that higher rate charging should increase polarization; thus noisier conditions in testing, and as the rate increases, it may result in rate-dependent causality in the disparity of state functions between the two electrodes in the cell.

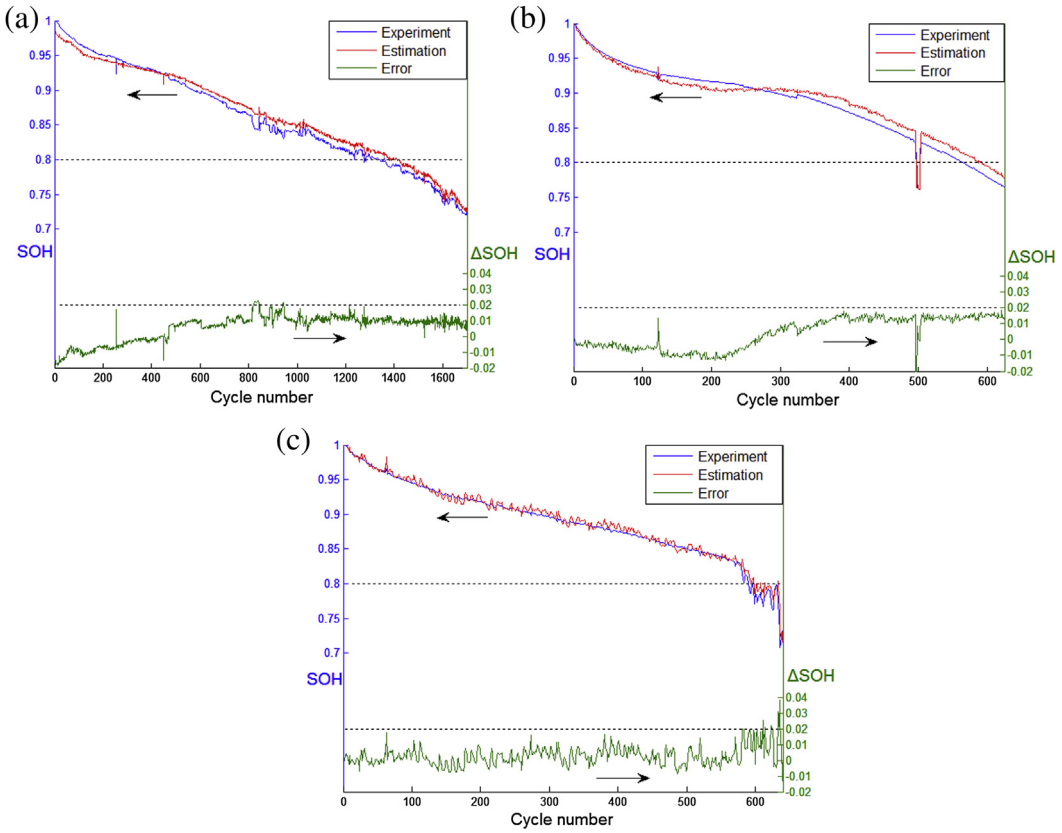

Fig. 3. The SOH estimation against experimental data and the error ($\Delta SOH = SOH_{est.} - SOH_{exp.}$) in each cycle estimated by using Eq. (14). Plots (a)–(c) are for batteries No. 1–3 respectively.

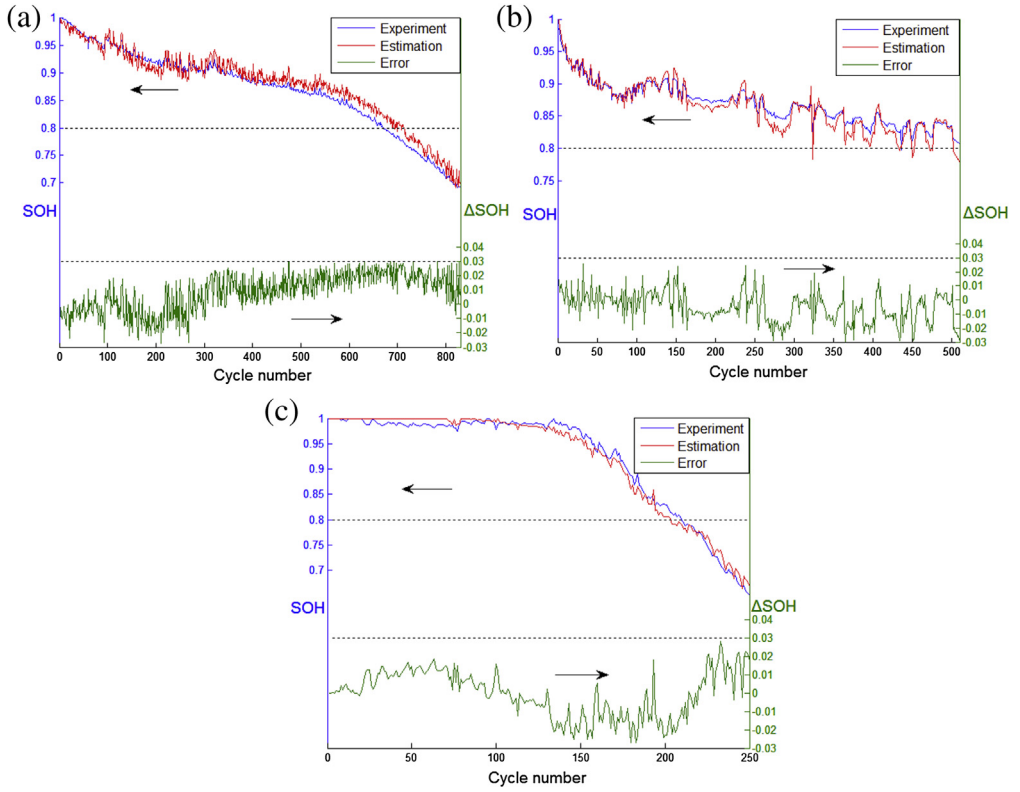

Fig. 4. The SOH estimation against experimental data and the error ($\Delta SOH = SOH_{est.} - SOH_{exp.}$) in each cycle was calculated by Eqs. 15–17, respectively. Plots (a)–(c) are for batteries No. 4–6, respectively.

Using graphite as the negative electrode as an example, the high rate charging could create rate limitation situations, or worse lithium deposition, on the negative electrode [14] and lead to a more severe degradation in cell performance. Such an influence on the accuracy of the model's predictability cannot be ignored. We thus suggest that a proper charging current (e.g. 0.5C) should be selected and preferred for SOH estimation, as the lower the rate the less the error and the better reliability should be received. Although we have not discussed the influences of aging and degradation mechanisms on the accuracy of the model prediction, it is a subject will be elaborated in our future work.

5. Conclusion

An SOH estimation method is illustrated here, which is based on a simple equivalent circuit modeling approach to parameterize a single-variable, time-based SOH inference model using CC charging profiles at various stages of life for the SOH estimation. The initial CC charging profile when a battery is commenced for service is benchmarked as 100% SOH. Subsequently, the SOH of the battery can be estimated by this inference model as the battery ages. The model parameters can be derived from a nonlinear least squares algorithm. The high accuracy of this SOH estimation approach was validated by experimental results using cells under different charging protocols and using cells with different sizes and chemistries. The simplicity of this method makes implementation easy for on-board applications, enjoying the benefits of less demand on prior learning and universality in application to different battery designs, chemistries, and operating conditions. Especially, this approach gives accurate SOH estimates irrelevant to duty schedules, making this approach attractive for practical applications.

Acknowledgment

This work is funded by Tsinghua National Laboratory for Information Science and Technology (TNList) Cross-discipline Foundation.

References

[1] D. Andre, C. Appel, T. Soczka-Guth, D. Uwe Sauer, J. Power Sources 224 (2013) 20–27.
[2] A. Widodo, M.-C. Shim, W. Caesarendra, B.-S. Yang, Expert Syst. Appl. 38 (2011) 11763–11769.
[3] H.-T. Lin, T.-J. Liang, S.-M. Chen, IEEE Trans. Ind. Inform. 9 (2) (2013) 679–685.
[4] A. Eddahech, O. Briat, N. Bertrand, J.-Y. Delétage, J.-M. Vinassa, Electr. Power Energy Syst. 42 (2012) 487–494.
[5] H.-T. Lin, T.-J. Liang, S.-M. Chen, in: IEEE 7th International Power Electronics and Motion Control Conference, Harbin, China, 2012, pp. 2678–2682.
[6] Y.-H. Chiang, W.-Y. Sean, J.-C. Ke, J. Power Sources 196 (2011) 3921–3932.
[7] B.Y. Liaw, R.G. Jungst, G. Nagasubramanian, H.L. Case, D.H. Doughty, J. Power Sources 140 (2005) 157–161.
[8] G.K. Prasad, C.D. Rahn, J. Power Sources 232 (2013) 79–85.
[9] S.J. Moura, N.A. Chaturvedi, M. Krsti&cacute, in: The 2012 American Control Conference, Montréal, Canada, 2012, pp. 566–571.
[10] J. Lee, O. Nam, B.H. Cho, I. Manda, J. Power Sources 174 (2007) 9–15.
[11] S. Abu-Sharkh, D. Doerffel, J. Power Sources 130 (2004) 266–274.
[12] J. Fan, S. Tan, J. Electrochem. Soc. 153 (6) (2006) A1081–A1092.
[13] M. Chen, G.A. . Rincón-Mora, IEEE Trans. Energy Convers. 21 (2) (2006) 504–511.
[14] B.K. Purushothaman, U. Landau, J. Electrochem. Soc. 153 (3) (2006) A533–A542.